

Soluble Polybenzimidazoles with Intrinsic Porosity: Synthesis, Structure, Properties and Processability

Vikas Kumar,^{1,2} Shyambo Chatterjee,¹ Pragati Sharma,^{2,3} Suman Chakrabarty,⁴ Chilukuri V. Avadhani ,¹ Swaminathan Sivaram^{1,5}

¹Polymer Science and Engineering Division, CSIR-National Chemical Laboratory, Dr. Homi Bhabha Road, Pune 411008, India

²Academy of Scientific and Innovative Research, Delhi-Mathura Road, New Delhi 110025, India

³Physical Chemistry Division, CSIR-National Chemical Laboratory, Dr. Homi Bhabha Road, Pune 411008, India

⁴School of Chemical Sciences, National Institute of Science Education and Research Bhubaneswar, P.O. Jatni, Khurda, Odisha 752050, India

⁵Indian Institute of Science Education and Research, Dr Homi Bhabha Road, Pune 411008, India

Correspondence to: S. Sivaram (E-mail: s.sivaram@iiserpune.ac.in)

Received 30 November 2017; accepted 28 January 2018; published online 00 Month 2018

DOI: 10.1002/pola.28979

ABSTRACT: We have explored two novel comonomers, namely, 4,16-dicarboxyl[2.2]paracyclophane and 5,5',6,6'-tetraamino-3,3,3',3'-tetramethyl-1,1'-spirobi[indane], for the synthesis of co-polybenzimidazoles (co-PBIs) with intrinsic porosity. Both these monomers possess twisted structures that can lead to “awkward” macromolecular shapes that cannot pack efficiently. The consequences of introducing these two monomers on the structure and properties of PBIs are reported. The random copolymers synthesized are amorphous and possess glass transition temperatures (T_g s) greater than 400 °C. T_g decreases with increasing comonomer content indicating an increase in fractional free volume. The copolymers have low surface area. TEM and BET measurements show evidence of

mesopore formation. The copolymers show significant carbon dioxide adsorption. Single chain molecular dynamics simulation of 24-mer repeat units shows intramolecular void spaces arising as a result of distorted polymer chain with reduced conformational mobility. These studies define a new synthetic strategy for “bottoms-up” synthesis of PBIs with intrinsic porosity. © 2018 Wiley Periodicals, Inc. *J. Polym. Sci., Part A: Polym. Chem.* **2018**, *00*, 000–000

KEYWORDS: bottoms-up synthesis; conformationally contorted monomers; CO₂ adsorption; high T_g polymers; heteroatom containing polymers; high temperature materials; mesoporous polymers; polybenzimidazole; polycondensation

INTRODUCTION Porous polymers are materials containing one or more types of pores, generally classified as microporous (having pores <2 nm), mesoporous (having pores between 2 and 50 nm), and macroporous (pores >50 nm).^{1,2} Pore geometry, pore size, pore surface, and polymer framework structure including composition and topology are important features that determine the property and applications of porous polymers. Porous polymers have attracted significant attention in recent years owing to their potential for applications in areas such as gas adsorption and storage, gas separations, and catalysis. Porosity in polymers can be built either at the time of its synthesis or using a variety of post polymerization methods.

Polymers with intrinsic microporosity (PIMs) are a special class of porous polymers which are synthesized using a “bottoms-up” approach and have found many useful

applications.^{3,4} Intrinsic microporosity in polymers is defined as “a continuous network of interconnected intermolecular voids, which form as a direct consequence of the shape and rigidity of the component macromolecules.”^{5,6} PIMs are amorphous materials having large and accessible surface area. PIMs are synthesized using monomers having rigid and contorted structures that restrict the degrees of conformational freedom available to the polymer chain. This limits their ability to pack efficiently resulting in high fractional free volume.⁷ The balance between intrachain rigidity and interchain spacing creates interconnected porous structures.

Polybenzimidazole (PBI) is a class of high-performance amorphous polymer which is receiving increasing attention in recent years due to their interesting structural framework, high thermal and chemical stability, unique functionality (*n*-electron donors), and ability to form strong hydrogen bond networks in presence of Bronsted acids.^{8–10} Many

Additional Supporting Information may be found in the online version of this article.

© 2018 Wiley Periodicals, Inc.

applications for PBIs in areas such as proton conducting membranes in high temperature fuel cells, nano-filtration, and other separation membranes have been reported.^{11–15}

However, there is far less information available in the literature on the preparation of porous PBIs. Macroporous PBIs were reported by casting a solution of PBI in dimethyl acetamide in presence of di-*n*-butyl phthalate as a porogen followed by removing the porogen using methanol.¹⁶ Cross-linked PBIs were prepared using an aromatic tricarboxylic acid and silica nanoparticles. Subsequently, silica nanoparticles were removed using 4 M ammonium bifluoride to yield a mesoporous network with a surface area of 190 m²/g, ~10 nm pore size, and void volume of 37%.¹⁷ A highly porous cross-linked polymer bearing a benzimidazole group has been reported via the condensation reaction of 2,3,6,7,10,11-hexaaminotriphenylene and tetrakis(4-formylphenyl)pyrene.¹⁷ The solid had a surface area exceeding 1100 m²/g. More recently, a “sponge like” porous PBI has been prepared using water vapor induced phase inversion and its application explored as a separator membranes in lithium ion battery.¹⁸

To the best of our knowledge, soluble PBIs with intrinsic porosities synthesized by a “bottoms-up” approach are not reported in the literature. We reasoned that such PBIs can be prepared using specially selected tetraamine or dicarboxylic acid comonomers with highly twisted structures that provide “awkward” macromolecular shapes that cannot pack efficiently. We chose two representative monomers for this purpose, namely, 4,16-dicarboxyl[2.2]paracyclophane and 5,5',6,6'-tetraamino-3,3',3'-tetramethyl-1,1'-spirobi[indane].

[2.2]Paracyclophane has the necessary structural features for accomplishing this goal.¹⁹ A characteristic feature of the cyclophane is the electronic interaction of the closely stacked π system (the distance between aromatic rings is between 2.8 and 3.1 Å) and the high amount of molecular strain which manifests itself in the distortion of the benzene rings into a boat shape. This results in characteristic spectroscopic features and leads to unusual effect on the reactivity of [2.2]paracyclophanes.^{20,21} Since cyclophane is a twisted structure, its incorporation into rigid glassy polymer network is expected to result in packing defects and creation of a high amount of free volume.²² Comonomers bearing a spiro tetrahedral carbon linkage (spirobisindanes) have been used for the preparation of PIMs, which exhibit microporosity and in, some instances, solubility with pore size ranging from 6 to 10 Å.^{23,24} It has been demonstrated that the spirobisindane unit is the site of contortion.^{25,26} The rigidity is enforced by the polymer being composed of fused rings and the nonlinear structure arises from the incorporation of spiro centers as “sites of contortion.”

We report here the synthesis of a cyclophane monomer, namely, 4,16-dicarboxyl[2.2] paracyclophane (**2**) and a spirobisindane monomer, 5,5',6,6'-tetraamino-3,3',3'-tetramethyl-1,1'-spirobi[indane] (**6**) capable of copolymerizing with 3,3'-diaminobenzidine and isophthalic acid to form copolymers of PBI and a study of the structure and properties of the resulting copolymers. The synthesis of the spirobisindane

monomer (**6**) is being reported for the first time. There is, however, one prior report on the preparation of PBIs using 3,3'-diaminobenzidine and 4,16-dicarboxyl[2.2]paracyclophane. The monomer as well as the insoluble polymer were poorly characterized.²²

EXPERIMENTAL

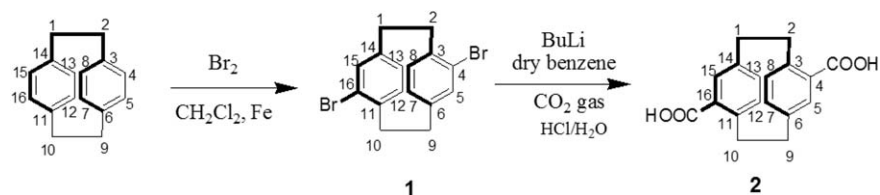
Materials

[2.2]Paracyclophane, 3,3'-diaminobenzidine, isophthalic acid, polyphosphoric acid, bisphenol A, and Pd/C 10 wt % were obtained from Aldrich and used as received. *N,N*-dimethyl acetamide (DMAc), methanesulfonic acid, hydrazine hydrate, potassium carbonate, dichloroacetamide, potassium iodide, and nitric acid were obtained from Thomas Baker (India) and used as received. *n*-Butyl lithium (2.5 M in hexane) was purchased from Alfa Aesar. Ethanol, methanol, acetic acid, dichloromethane, and sodium hydrogen carbonate were obtained from Hi Media (Mumbai, India) and used as received. Deionized water was used in all experiments.

Characterization

Fourier transform infrared spectra were recorded on a Perkin-Elmer Spectrum GX spectrometer. The polymer IR spectra were recorded using a film (thickness ~15 μ) in an ATR mode. ¹H- and ¹³C-NMR spectra were recorded on a Bruker-AV 500 MHz spectrometer with tetramethylsilane as an internal standard and CDCl₃ or DMSO-*d*₆ as a solvent. HRMS analysis was carried out on Thermo Scientific Q-Exactive instrument. Thermal stability of polymers was investigated by thermogravimetric analysis on Perkin Elmer: STA 6000 instrument and was conducted in nitrogen at a heating rate of 10 °C min⁻¹ from 50 to 900 °C. Glass transition temperatures (*T*_g) were obtained from DSC (TA Q-10 model) with a heating rate of 10 °C min⁻¹ under nitrogen atmosphere. *T*_g of the polymers was determined from the second heating cycle. TEM images were recorded using a Technai-300 instrument by dispersing the powdered polymer sample in ethanol on a Formvar-copper grid. X-Ray diffraction analysis was performed on Rigaku MicroMax-007HF X-ray diffractometer at 40 kV and 30 mA. The single crystal data was collected using Bruker SMART APEX II single crystal X-ray CCD diffractometer with graphite-monochromatised (Mo- $K\alpha$ = 0.71073 Å) radiation. Inherent viscosity was measured in an Ubbelohde Viscometer in 98% sulfuric acid (0.2 wt %) at 30 ± 0.1 °C. BET surface area of polymers was determined by N₂ adsorption at 77 K. CO₂ uptake was determined at 273 K using Quantachrome Quadrasorb automatic volumetric instrument. Polymer powder was activated under high vacuum at 150 °C for 8 h before measurements.

Molecular dynamics simulations were performed to deduce the energetically most favorable structural conformations. An all-atomistic model was used. Gromacs Package 1 and OPLS-AA2 force field were used. A chain length of 24 repeat units was taken for simulations, which were performed in NVT ensemble at 800 K and 1 bar. Temperature was ~50–60 K above the *T*_g of PBI so as to ensure better sampling of polymer conformations.



SCHEME 1 Synthesis of 4,16-dicarboxyl[2.2]paracyclophane (**2**).

Synthesis of 4,16-Dibromo[2.2]paracyclophane (**1**)

Synthesis of 4,16-dibromo[2.2]paracyclophane was carried out as per reported procedure.²² [2.2]Paracyclophane (3 g, 0.014 mol) was stirred with 30 mL of methylene chloride in a nitrogen atmosphere. Bromine (4.6 g, 0.028 mmol) was added in several portions. The colored solution was stirred for 72 h at room temperature and then poured into water. The aqueous layer was extracted with methylene chloride. The combined organic layers were washed with water, dried, and the solvent removed. The crude solid was washed with dichloromethane several times until the orange color disappeared. The resulting white solid was dissolved in CH₂Cl₂ and the solution evaporated slowly at room temperature. After 1 day, a crystalline solid was formed which was separated by filtration. [Structure of **1** (CCDC number: CCDC 1574723); (CIF) Check CIF file (pdf)]

Yield of **1**: 2.1 g (40%), mp 245 °C (Lit²² mp 250 °C). ¹H-NMR (500 MHz, CDCl₃): δ 7.2 (dd, 2 H), 6.61 (m, 4 H), 3.52–2.92 (m, 8 H). ¹³C-NMR (500 MHz, CDCl₃): δ 141.04, 138.93, 136.72, 134.13, 130.81, 128.25, 35.35, 33.47.

Synthesis of 4,16-Dicarboxyl[2.2]paracyclophane (**2**)

The synthesis of **2** was carried out according to a reported procedure.²² A mixture of 4,16-dibromo[2.2]paracyclophane (0.2 g) and dry benzene (20 mL) was placed in a dry, three-necked flask equipped with a condenser, CaCl₂ guard tube, a magnetic stirrer, and a nitrogen gas inlet. *n*-Butyl lithium (2.5 M, 10 mL) was added via a syringe. The resulting mixture was heated to reflux for 5 h under nitrogen atmosphere. Dry CO₂ gas was bubbled through the hot reaction mixture. The orange milky mixture changed to an off white milky precipitate. The precipitate was allowed to cool to room temperature. The precipitate was acidified with hydrochloric acid solution (3 mL HCl + 7 mL H₂O). The acidified solution was filtered to obtain a white product.

Yield of **2**: 0.037 g (23%), mp: 410 °C. ¹H-NMR (500 MHz, DMSO-*d*₆): δ 7.01 (s, 2H), 6.58 (d, *J* = 10 Hz, 2H), 6.43 (d, *J* = 10 Hz, 2H), 3.03–2.82 (m, 8H). ¹³C-NMR (500 MHz, DMSO-*d*₆): δ 170.73, 141.83, 139.63, 136.06, 135.01, 133.57, 34.93, 34.45.

Synthesis of 6,6'-Dihydroxy-3,3,3',3'-tetramethyl-1,1'-spirobi[indane] (**3**)

Synthesis of **3** was performed according to a previously reported procedure.²⁵ Bisphenol A (30 g, 0.1315 mol) and methane sulfonic acid (3.5 mL) were taken in a 250-mL round-bottomed flask and the mixture was stirred at 140 °C for 4 h. The brown sticky oily mixture was poured into

warm water (1 L) with continuous stirring. The mixture was washed several time with water until neutral pH and dried at 100 °C in a vacuum oven for 1 day. The compound was purified by the crystallization from pet ether and ethyl acetate in (70/30) mixture.

Yield of **3**: 18 g (40%), mp: 210–212 °C (Lit²⁷: 215.5–217 °C). ¹H-NMR (500 MHz, DMSO-*d*₆): δ 9.03 (s, 2H), 7.00 (d, 2H), 6.6 (dd, 2H), 6.09 (d, 2H), 2.26 (d, 2H), 2.1 (d, 2H), 1.3 (s, 6H), 1.24 (s, 6H). ¹³C-NMR (500 MHz, DMSO-*d*₆): δ 158.81, 151.55, 142.21, 127.3, 114.42, 109.99, 59.4, 59.97, 42.39, 31.69, 30.53. FT IR (KBr, cm⁻¹): 3167–3292 (str O–H), 2985 (str CH₃), 1617 (str CH₂).

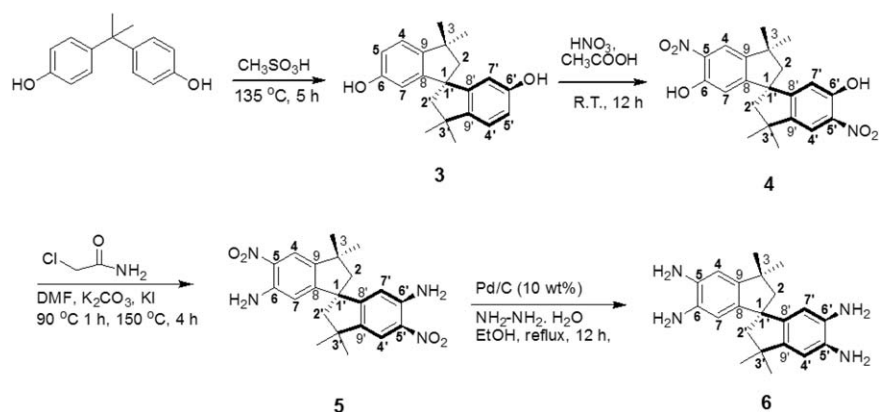
Synthesis of 6,6'-Dihydroxy-3,3,3',3'-tetramethyl-5,5'-dinitro-1,1'-spirobi[indane] (**4**)

Synthesis of **4** was achieved following a reported procedure.²⁵ Into a 250-mL round-bottomed flask, compound **3** (10 g, 0.03 mol) and acetic acid (50 mL) were added and stirred. To this, a mixed solution of nitric acid (4 N, 2.1 equivalents, 18 mL) and acetic acid (50 mL) was added drop wise and stirred overnight. The mixture was cooled and poured into water, filtered, and dried at 100 °C in vacuum oven for 1 day. A light yellowish powder was isolated by column chromatography (pet ether: ethyl acetate: 90/10, v/v).

Yield of **4**: 3g (25%), mp: 230–233 °C (Lit²⁸: 238–241 °C). ¹H-NMR (500 MHz, CDCl₃): δ 10.59 (s, 2H), 7.9 (s, 2H), 6.52 (s, 2H), 2.45 (d, 2H), 2.27 (d, 2H), 1.43 (d, 12H). ¹³C-NMR (500 MHz, CDCl₃): δ 162.19, 157.18, 148.55, 142.07, 124.01, 118.78, 63.5, 62.7, 48.18, 36.3, 35.04. FT IR (KBr, cm⁻¹): 3167–3292 (str O–H), 2985 (str CH₃), 1548 (asym str NO₂), 1378 (sym str NO₂), 1617 (str CH₂).

Synthesis of 6,6'-Diamino-3,3,3',3'-tetramethyl-5,5'-dinitro-1,1'-spirobi[indane] (**5**)

Into a three-necked 100 mL round-bottomed flask equipped with a nitrogen inlet, calcium guard tube, and a reflux condenser was added **4** (1.393 g, 3.5 mmol) and freshly distilled DMF (15 mL) and the mixture was stirred for 15 min at room temperature to get a clear, homogenous solution. To this, potassium carbonate (4.3 g, 30 mmol) was added and stirred for 15 min. 2-Chloroacetamide (1.57 g, 12.6 mmol) and potassium iodide (KI) (0.464 g, 2.8 mmol) were added and the mixture was heated at 90 °C for 1 h and then at 150 °C for 4 h. At the end of the reaction, the mixture was poured into water and extracted with dichloromethane. The organic layer was collected, dried over anhydrous sodium sulfate, and concentrated. The crude compound was purified by column chromatography (pet ether/ethyl acetate: 90/10, v/v).



SCHEME 2 Synthesis of 5,5',6,6'-tetraamino-3,3,3',3'-tetramethyl-1,1'-spiro[indane] (**6**).

Yield of **5**: 0.45 g (32%); mp: 303–306 °C. $^1\text{H-NMR}$ (500 MHz, CDCl_3): δ 7.93 (s, 2H), 6.24 (s, 2H), 5.97 (s, 4H), 2.40 (dd, 4H), 1.41 (d, 12H). $^{13}\text{C-NMR}$ (500 MHz, CDCl_3): δ 159.36, 144.84, 142.44, 132.46, 119.51, 113.39, 59.0, 57.66, 43.06, 31.59, 30.19. FT IR (KBr, cm^{-1}): 3372 (str N—H), 1635 (bend N—H), 1276 (str, C—N), 2983 (str CH_3), 1554 (asym str NO_2), 1383 (sym str NO_2), 1613 (str CH_2). HRMS: calcd for $\text{C}_{21}\text{H}_{25}\text{N}_4\text{O}_4^+ [\text{M} + \text{H}]^+$: 397.18; found: 397.18.

Synthesis of 5,5',6,6'-Tetraamino-3,3,3',3'-tetramethyl-1,1'-spiro[indane] (**6**)

Into a three-necked 100 mL round-bottomed flask equipped with a nitrogen inlet a reflux condenser and calcium guard tube was added **5** (0.396 g, 1.0 mmol) and ethanol (20 mL) and stirred for 15 min. Pd/C (10 wt %) (40 mg) and hydrazine hydrate (4 mL) was added and refluxed overnight at 70 °C. The mixture was cooled to room temperature and poured into ice water. The precipitated compound was filtered and dried in a vacuum oven at 100 °C for 24 h.

Yield of **6**: 0.315 g (94%); mp: 241–243 °C. $^1\text{H-NMR}$ (500 MHz, CDCl_3): δ 6.52 (s, 2H, Ar—H), 6.20 (s, 2H, Ar—H), 3.22 (s, 8H, — NH_2), 2.28 (dd, 4H, — CH_2), 1.33 (d, 12H, — CH_3). $^{13}\text{C-NMR}$ (500 MHz, CDCl_3): δ 144.42, 142.85, 134.07, 112.38, 109.74, 59.84, 42.88, 31.74, 30.51. FT IR (KBr, cm^{-1}): 3341 (str N—H), 1619 (bend N—H), 1267 (str, C—N), 2986 (str CH_3), 1619 (str CH_2). HRMS: calcd for $\text{C}_{21}\text{H}_{29}\text{N}_4^+ [\text{M} + \text{H}]^+$: 337.24; found: 337.23.

Synthesis of PBIs from 3,3'-Diaminobenzidine and isophthalic acid (**7**)

A 100-mL three-necked round-bottomed flask equipped with a N_2 inlet, mechanical stirrer, and a CaCl_2 drying tube was charged with 120 g of polyphosphoric acid and heated to 100 °C and stirred for 1 h. 3,3'-Diaminobenzidine (3 g, 14.0 mmol) was added slowly and the temperature was raised to 120 °C and maintained for 1 h. Isophthalic acid (2.32 g, 14.0 mmol) was added slowly. The temperature was increased to 170 °C and maintained for 5 h and then at 210 °C for 16 h. The reaction mixture was allowed to cool and poured into

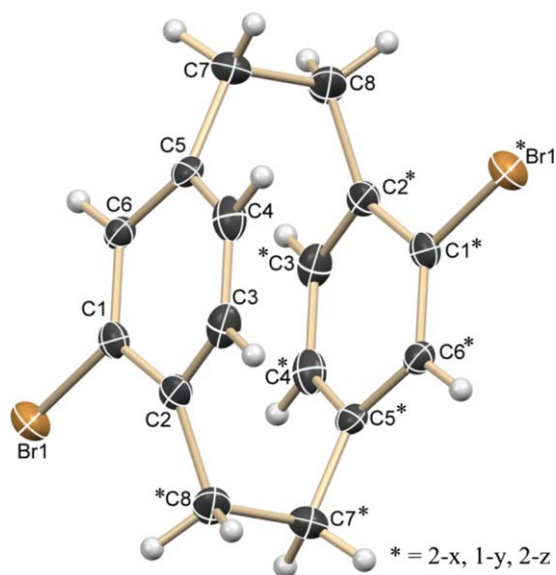


FIGURE 1 ORTEP diagram of 4,16-dibromo[2.2]paracyclophane. [Color figure can be viewed at wileyonlinelibrary.com]

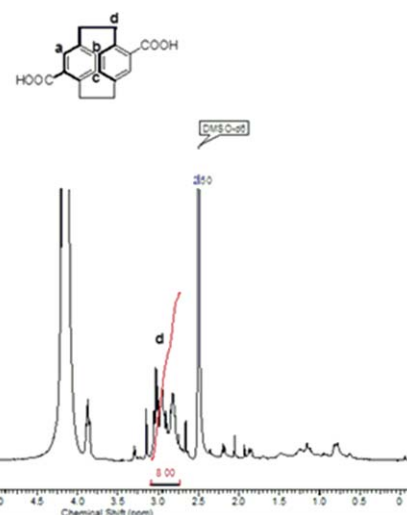


FIGURE 2 $^1\text{H-NMR}$ (DMSO-d_6) spectrum of 4,16-dicarboxyl[2.2]paracyclophane (**2**). [Color figure can be viewed at wileyonlinelibrary.com]

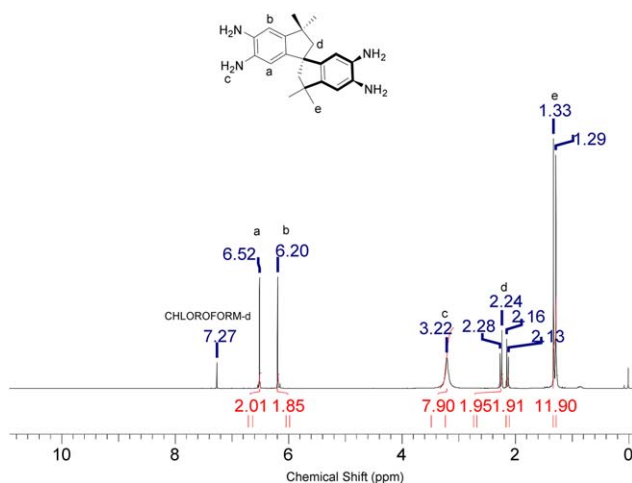


FIGURE 3 $^1\text{H-NMR}$ (CDCl_3) spectrum of **6**. [Color figure can be viewed at wileyonlinelibrary.com]

1 L of water. The precipitated polymer was washed with copious amounts of water followed by 10% sodium carbonate until the filtrate was neutral. The polymer was filtered, washed with acetone, and dried at 100 °C for 48 h.

Yield: 5.2 g (98% conversion). $^1\text{H-NMR}$ (500 MHz, $\text{DMSO-}d_6$): δ 13.26 (s, 2 H), 9.15 (s, 1H), 8.33 (d, 2 H), 7.8–7.65 (m, 7 H). $^{13}\text{C-NMR}$ (500 MHz, $\text{DMSO-}d_6$): δ 151.27, 136.57, 131.36, 130.29, 127.85, 125.28. FT IR (Film, cm^{-1}): 2953–3573 (str N–H), 1612 (str, C–N), 1536 (in-plane deformation of benzimidazole) and 1286 (breathing mode of benzimidazole).

Synthesis of Co-PBIs with 5 Mol % 4,16-Dicarboxyl[2.2]paracyclophane (**2**), 3,3'-Diaminobenzidine, and Isophthalic Acid (**8a**)

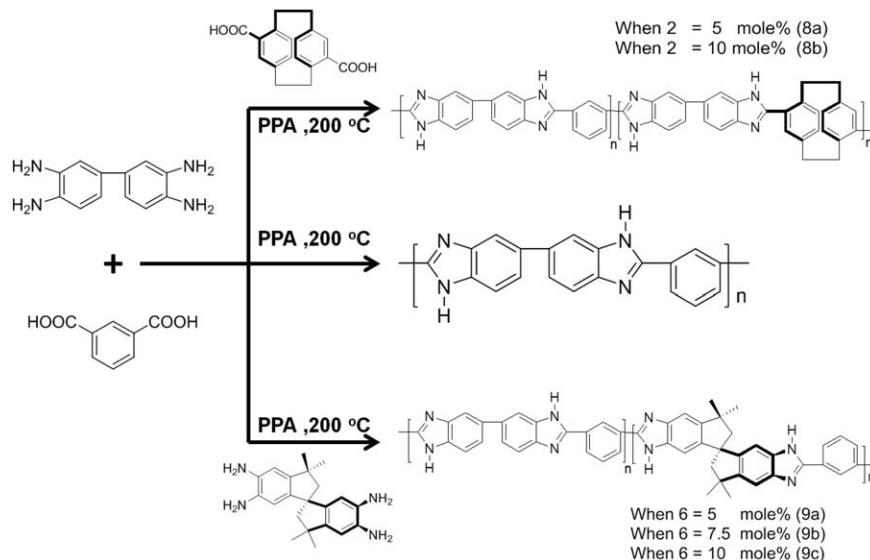
A 100-mL three-necked round-bottomed flask equipped with a N_2 inlet, mechanical stirrer and a CaCl_2 drying tube was charged with 35 g of polyphosphoric acid and heated to

100 °C and stirred for 1 h. 3,3'-Diaminobenzidine (1g, 4.67 mmol) was added slowly and the temperature was increased to 120 °C and maintained for 1 h. Isophthalic acid (0.702g, 4.44 mmol) and 4,16-dicarboxyl[2.2]paracyclophane (**2**) (0.067 g, 0.23 mmol, 5 mol %) was added slowly. The temperature was increased to 170 °C and maintained for 5 h and then at 210 °C for 16 h. The reaction mixture was allowed to cool and poured into 700 mL water. The precipitated polymer was washed with copious amounts of water followed by 10% sodium carbonate until the filtrate was neutral. The polymer was filtered, washed with acetone, and dried at 100 for 48 h. Yield of **8a**: 1.615 g (91% conversion).

Copolymer containing 10 mol % **2** (**8b**) was prepared in a similar manner. Yield: of **8b** 1.69 g (94% conversion). $^1\text{H-NMR}$ (**8b**) (500 MHz, $\text{DMSO-}d_6$): δ 13.25 (s, 2 H), 9.15 (s, 1H), 8.33 (s, 2 H), 8.04–7.65 (m, 7 H), 2.17–1.91 (m, 8 H of 10 mole% **2**, $-\text{CH}_2$). $^{13}\text{C-NMR}$ (**8b**) (500 MHz, $\text{DMSO-}d_6$): δ 151.87, 136.71, 131.44, 130.24, 127.96, 125.26. FT IR (**8b**) (Film, cm^{-1}): 2958–3389 (str N–H), 1618 (str, C–N), 1527 (in-plane deformation of benzimidazole) and 1268 (breathing mode of benzimidazole).

Synthesis of Co-PBIs with 5 Mol % 5,5',6,6'-Tetraamino-3,3,3',3'-tetramethyl-1,1'-spirobi[indane] (**6**), 3,3'-Diaminobenzidine, and Isophthalic Acid (**9a**)

A 100-mL three-necked round-bottomed flask equipped with a N_2 inlet, mechanical stirrer, and a CaCl_2 drying tube was charged with 30 g of polyphosphoric acid and heated to 100 °C and stirred for 1 h. 3,3'-Diaminobenzidine (0.950 g, 4.44 mmol) and comonomer **5** (0.077 g, 0.23 mmol, 5 mole%) were added slowly and the temperature was increased to 120 °C and maintained for 1 h. Isophthalic acid (0.775 g, 4.67 mmol) was added slowly. The temperature was increased to 170 °C and maintained for 5 h and then at 210 °C for 16 h. The reaction mixture was allowed to cool and poured into 700 mL water. The precipitated polymer



SCHEME 3 Synthesis of PBI (**7**) and co-PBIs (**8a-b** and **9a-c**).

TABLE 1 Properties of Homo- and Co-PBIs

Polymer Sample (Comonomer and Content of Comonomer)	Inherent Viscosity (dL/g) in H ₂ SO ₄ at 30 ± 0.5 °C	% Weight Loss at 500 °C	% Weight Loss at 800 °C	% Char Yield	T _g (°C)	R _g (nm)
7 (None)	1.41	14	28	72	446	1.07
7a (Comonomer 6) ^a	–	–	–	–	–	1.36
7b (Comonomer 2) ^a	–	–	–	–	–	1.23
8a (2 , 5 mol %)	0.59	16	32	67	428	1.18
8b (2 , 10 mol %)	0.51	11	27	73	412	1.12
9a (6 , 5 mol %)	0.63	10	27	73	432	1.19
9b (6 , 7.5 mol %)	0.57	9	26	74	425	Not calculated
9c (6 , 10 mol %)	0.54	15	30	70	408	1.14

^a These polymers were not synthesized.

was washed with copious amounts of water followed by 10% sodium carbonate until the filtrate was neutral. The polymer was filtered, washed with acetone, and dried at 100 for 48 h. Yield of **9a**: 1.7 g (94% conversion).

Copolymers containing 7.5 mol % and 10 mol % **6** (**9b** and **9c**, respectively) were prepared in a similar manner. Yield of **9b**: 1.705 g (94% conversion) and **9c**: 1.736 g (95% conversion). ¹H-NMR (**9c**) (500 MHz, DMSO-*d*₆): δ 13.28 (s, 2 H), 9.17 (s, 1 H), 8.35 (s, 2 H), 7.93–7.66 (m, 7 H), 2.1 (d, 4 H of 10 mole% **6**, –CH₂), 1.51 (d, 12 H of 10 mole% **6**, –CH₃). ¹³C-NMR (**9c**) (500 MHz, DMSO-*d*₆): δ 151.84, 136.84, 131.43, 130.21, 128.02, 125.23, 122.72, 119.47, 117.61, 112.6, 109.86, 32.52, 31.13, 24.91, 21.81. FT-IR (**9c**) (film

cm⁻¹): 2938–3217 (str N–H), 1619 (str, C–N), 1538 (in-plane deformation of benzimidazole) and 1285 (breathing mode of benzimidazole).

Preparation of Films

Polymer (0.3 g) was dissolved at 80 °C in 10 mL of DMAc. The solution was stirred overnight and filtered before being cast on a clean glass plate. The solvent was evaporated at 90 °C overnight under nitrogen and then heated gradually to 200 °C and maintained at this temperature for 1 h. After cooling to room temperature, the membrane was peeled off from the glass plate by immersion in water and dried under high vacuum for 5 h at 120 °C.

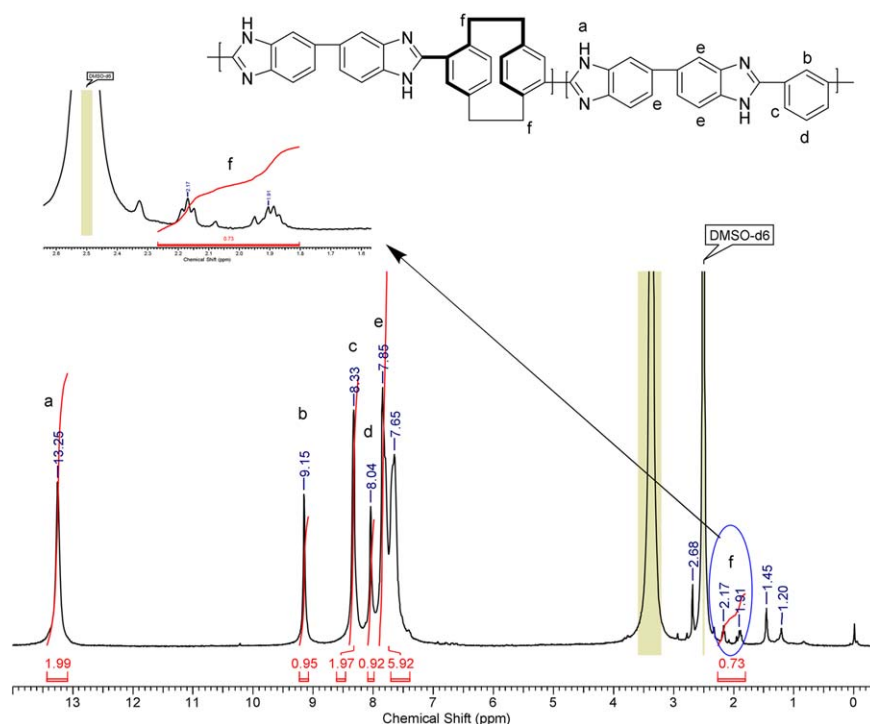


FIGURE 4 ¹H-NMR (DMSO-*d*₆) spectrum of **8b** containing 10 mol % **2**. [Color figure can be viewed at wileyonlinelibrary.com]

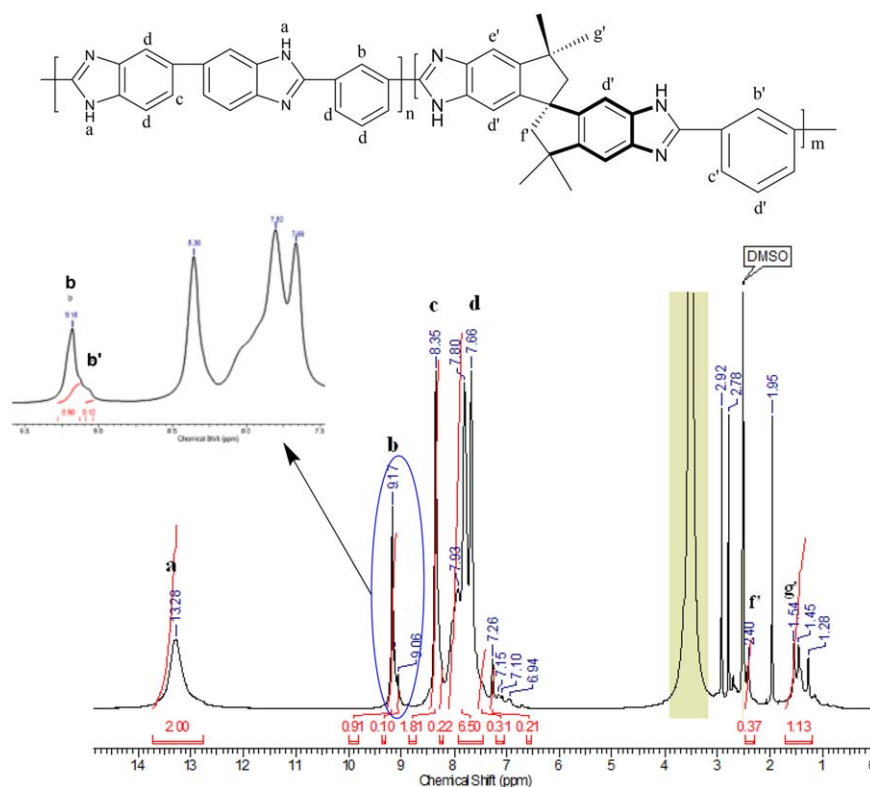


FIGURE 5 ^1H NMR (DMSO-d_6) spectrum of **9c** containing 10 mol % **6**. [Color figure can be viewed at wileyonlinelibrary.com]

RESULTS AND DISCUSSION

Synthesis of Monomers

Two monomers, namely, 4,16-dicarboxyl[2.2]paracyclophane (**2**) and 5,5',6,6'-tetraamino-3, 3',3'-tetramethyl-1,1'-spirobi[indane] (**6**), were synthesized as shown in Schemes 1 and 2, respectively.

Electrophilic bromination of [2.2]paracyclophane was performed as described by Cram and Cram.²⁰ Reactions performed using 2 equivalents of bromine yielded 4,16-dibromo[2.2]paracyclophane (**1**) along with several other isomers. However, the desired isomer could be crystallized in high purity from the mixture of products. The ^1H - and ^{13}C -NMR spectra of **1** are shown in Supporting Information Figures S1 and S2, respectively. The isomeric purity and the 4–16 orientation of the bromine in the phenyl ring of **1** was established by the single crystal X-ray structure (Fig. 1; Supporting Information Table S1).

4,16-Dicarboxyl[2.2]paracyclophane (**2**) was obtained by the carboxylation of the organolithium derivative of 4,16-dibromo[2.2]paracyclophane and subsequent acidification with HCl. The ^1H -NMR spectrum of compound **2** is shown in Figure 2.

Monomer **6** was synthesized by nitration of **3** followed by Smiles Rearrangement of the intermediate **4** to **5**. The ^1H - and ^{13}C -NMR spectra of **5** are shown in Supporting Information Figures S3 and S4. Activated aromatic hydroxyl group is transformed into the amino group during Smiles

rearrangement.²⁹ Structure of **6** was confirmed by ^1H -, ^{13}C -NMR and mass spectrometry. The ^1H -NMR spectrum of **6** is shown in Figure 3, while the ^{13}C -NMR spectrum of **6** is shown in Supporting Information Figure S5.

Synthesis, Structure, and Composition of Co-PBIs

PBI, homo, and copolymers were prepared by the reaction of 3,3'-diaminobenzidine, isophthalic acid, and comonomer **2** or **6** (Scheme 3) following the procedure reported in the literature.¹³ ^1H -NMR spectrum of PBI (**7**) is shown in Supporting Information Figure S6 and is in agreement the spectrum reported in the literature. PBI is soluble in polar solvents like DMAc, NMP, and DMSO. To ensure that the copolymers remain soluble, we restricted the comonomer content in the polymer to <10 mol %. The copolymers were also found to be soluble in DMAc, NMP, and DMSO at 25 °C. Inherent viscosity of the polymers was determined in 98 wt % H_2SO_4 and was found to be 1.41, 0.59, 0.51, 0.63, 0.57, and 0.54 dL/g for polymer **7**, **8a-b**, and **9a-c**, respectively (Table 1).

Comonomer content in the polymer was estimated from ^1H -NMR spectra and found to be in reasonable agreement with the feed composition. ^1H -NMR spectrum (Fig. 4) of copolymer **8b** show peaks at δ 2.17 and 1.91 ppm corresponding to the eight aliphatic protons of the paracyclophane ring with a unit of integration 0.73. Based on this, we can estimate the content of comonomer **2** in polymer **8b** to be about 9 mol %. The ^1H -NMR spectrum (Fig. 5) of **9c** shows a chemical shift at δ 13.28 ppm that is assigned to the two-imidazole protons. The chemical shift at δ 9.17 ppm is

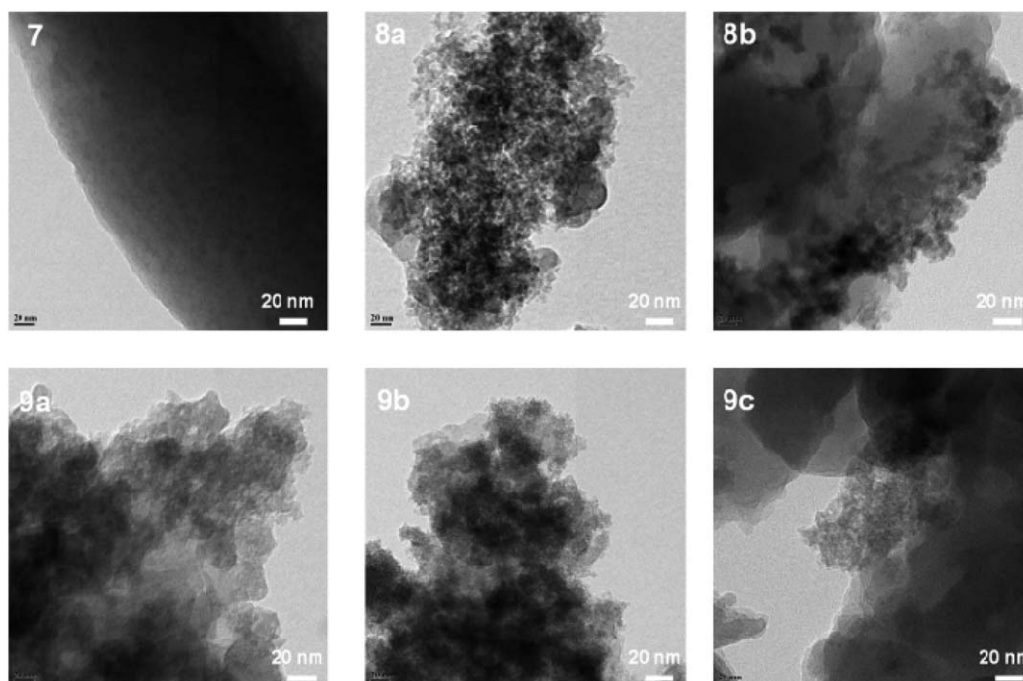


FIGURE 6 HR-TEM images of PBI **7** and copolymers, **8a-b** and **9a-c**.

attributed to the one aromatic proton of isophthalic acid marked as b. Copolymer **9c** exhibits a chemical shift for the same proton at δ 9.06 ppm (marked as b') with a unit of integration 0.1. Based on this, we estimate that the content of comonomer **6** in **9c** to be 10 mol %. Therefore, we conclude that the incorporation of the comonomers in the co-PBIs is near quantitative.

WAXD, T_g , and Thermogravimetric Analysis of Co-Polybenzimidazoles

All copolymers synthesized were found to be amorphous in nature (Supporting Information Fig. S7). In contrast to the homopolymer PBI, the copolymers show multiple broad peaks. Polymers **8a** and **9a** exhibit three peaks at $2\Theta = 14$, 18 , and 25° . However, polymers **8b** and **9c** which have ~ 10 mol % of the comonomers show only a broad peak at $2\Theta = 25^\circ$. Peak at $2\Theta = 25^\circ$ has been previously observed for amorphous PBI copolymers.^{30,31} The differential scanning calorimetry (DSC) data show that all polymers have high T_g , greater than 400°C (Supporting Information Fig. S8). Progressive increase in the comonomer content results in a decrease in T_g (Table 1). Decreasing T_g with increasing content of conformationally rigid, non-planar, and contorted comonomers can be attributed to the increase in the fractional free volume of the copolymer. All the co-PBIs are random in nature as shown by a satisfactory linear fit with the Flory-Fox equation (Supporting Information Figs. S9 and S10).

The thermogravimetric analysis of the synthesized polymers is shown in Supporting Information Figure S11. All polymers show $<15\%$ loss in weight at 500°C and less than 30% weight loss at 800°C under nitrogen. The char yield is about

$70 \pm 3\%$. These results are in agreement with what is generally reported for the PBI family of polymers in the literature.

TEM Analysis

All the synthesized samples were subjected to high-resolution transmittance electron microscopic analysis (Fig. 6). The homopolymer shows a layered structure without any appreciable porosity. The co-PBIs containing varying contents of comonomers exhibit a sponge like porous structure.

Surface Area and Porosity Measurements

The surface area and porosity of the synthesized polymers were investigated by physisorption of nitrogen at 77 K . The isotherms show nitrogen uptake at 1 bar pressure indicative of porous nature of the PBIs. The specific surface area and

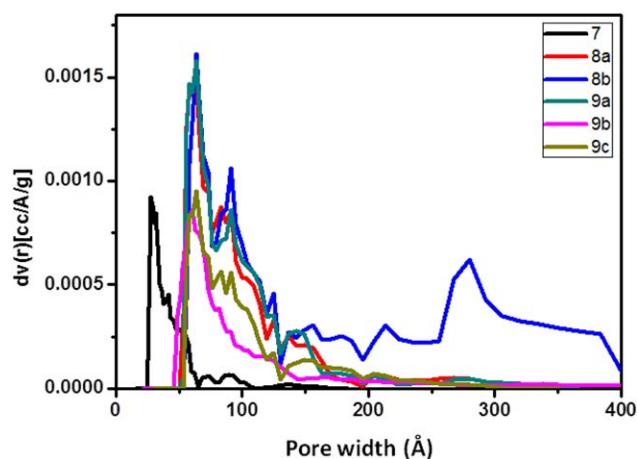


FIGURE 7 Pore size distribution curves for polymers **7**, **8a-b**, and **9a-c**. [Color figure can be viewed at wileyonlinelibrary.com]

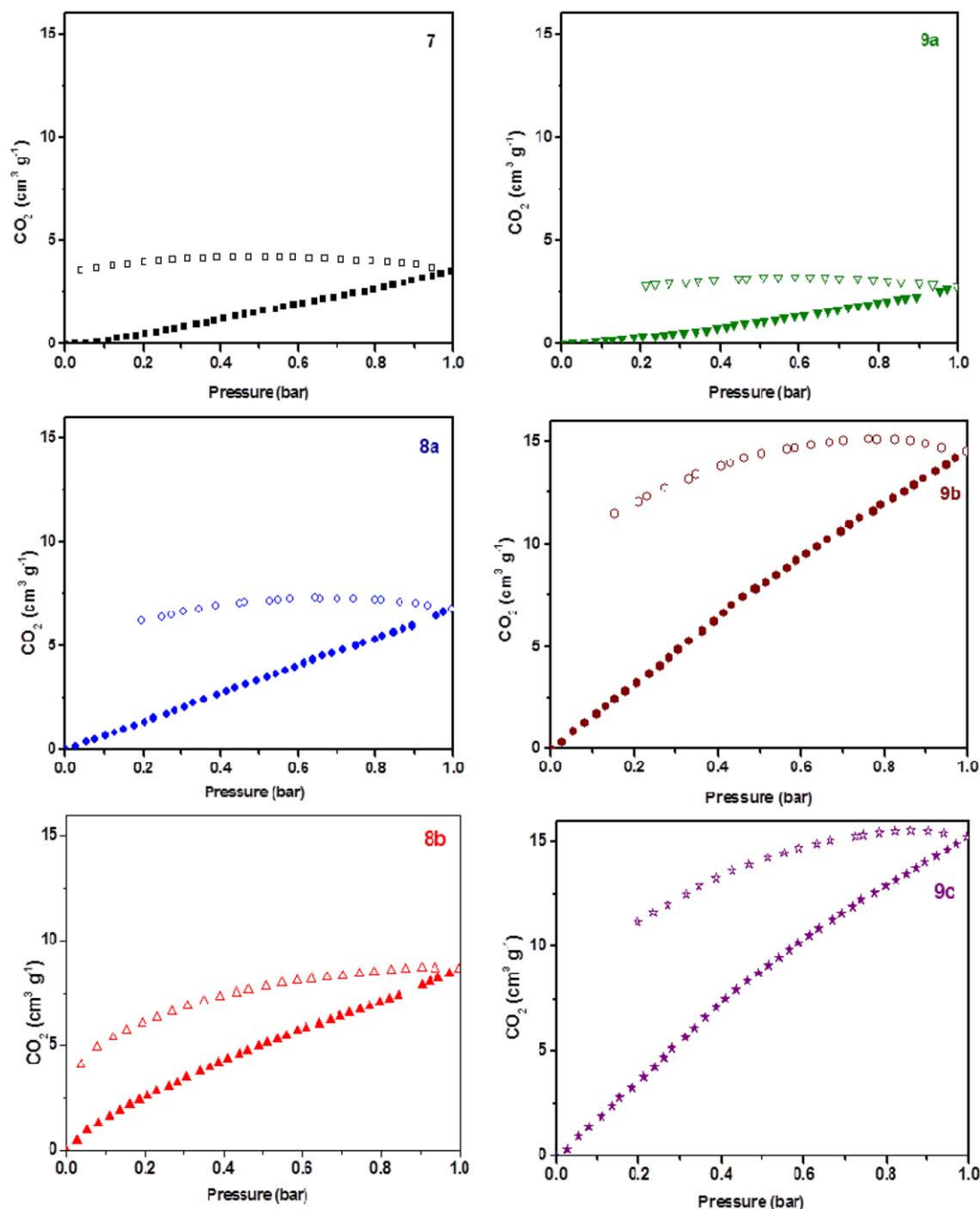


FIGURE 8 CO₂ adsorption and desorption behavior for polymers **7**, **8a-b**, and **9a-c**. [Color figure can be viewed at wileyonlinelibrary.com]

pore size were estimated from the adsorption and desorption isotherms and are shown in Supporting Information Figure S12. The measured BET surface area for the samples **8a-b** and **9a-c** are low, only around 10 m²/g. It is worth noting that the polymers reported here are copolymers containing only a small amount of comonomer. Apparently, at such low comonomer contents, its influence on surface area is limited. Most of the PIMs reported in the literature are homopolymers containing large amounts of conformationally rigid monomers whose influence on surface area is substantial.

The physisorption isotherms observed for polymers **7**, **8a**, **9a**, and **9b** (Supporting Information Fig. S12) show a slow and gradual increase in nitrogen uptake up to a relative pressure $P/P_0 = 1.0$, reminiscent of type III isotherms.³² It is believed that in such isotherms adsorbate-adsorbent interactions play an important role. Nitrogen adsorption isotherms of polymers **8b** and **9c** exhibit a slight variation in the nature of adsorption-desorption curves. The adsorption isotherms show a gradual increase in middle level relative pressures and a steeper increase at higher pressures. Such a

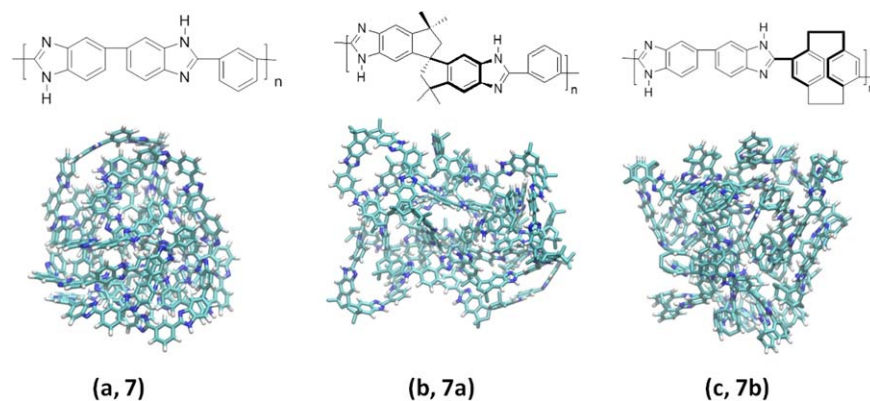


FIGURE 9 Molecular dynamics simulation of (a) isophthalic based PBI (**7**), (b) 5,5',6,6'-tetraamino-3,3,3',3'-tetramethyl-1,1'-spiro-bi[indane] (**6**) based PBI (**7a**), and (c) 4,16-dicarboxyl[2.2]paracyclophane (**2**) based PBI (**7b**). [Color figure can be viewed at wileyonlinelibrary.com]

behavior has earlier been reported as characteristic of mesopores.³³ There are several reports in the literature of porous and insoluble PBI networks which exhibit a type I adsorption isotherm which has been taken as evidence for dominant microporosity.^{34–36} The adsorption hysteresis appears to exhibit an H3 type behavior and is often associated with aggregates of plate-like particles giving rise to slit-shaped pores.³² The weak hysteresis observed can be understood either in terms of poor access of nitrogen molecule into narrow pore openings³⁴ or the powdery nature of samples.³⁵ The hysteresis curves also show that all adsorbed nitrogen is not fully desorbed indicating irreversible uptake of nitrogen in pores.

Pore size distribution was estimated by fitting the uptake branches of the nitrogen isotherms with nonlocal density functional theory and was found to be between 6 and 9 nm (Fig. 7). Polymer **8b** showed a distinct population of larger pores, approximately 28 nm. These results indicate that this method of synthesis does not provide adequate control over pore sizes.

Carbon Dioxide Adsorption Isotherm

Porous PBIs and polyimides have been previously explored as sorbents for carbon dioxide.^{33–37} Therefore, we subjected the polymers to CO₂ adsorption/desorption studies by measuring the sorption isotherms at 273 K under 1 bar pressure. The results are shown in Figure 8. Co-polymers **8a** and **9a** show similar behavior with low CO₂ adsorption at 1 atm pressure. Co-polymers **8b**, **9b**, and **9c** exhibit stronger CO₂ adsorption with an almost continuous uptake of CO₂ with pressure. The saturation has not been reached at 1 atm pressure. Contrary to this observation, most of the earlier studies of CO₂ absorption report a typical convex adsorption curve with little or no hysteresis.^{33,35,36} In the case of co-PBIs, the adsorption–desorption isotherms show significant hysteresis, indicating retention of residual CO₂ in the polymer. This phenomenon may be associated with the swelling of the porous structure or an irreversible chemical interaction of the adsorbate with the adsorbent. Earlier studies have reported

a range of CO₂ adsorption capacities, from about 10 to 22.5% depending on the nature of the polymer. The CO₂ adsorption capacities for polymer **7**, **8a**, **8b**, **9a**, **9b**, and **9c** were 0.7%, 1.3%, 1.7%, 0.5%, 2.9%, and 3.0%, respectively. It must be recognized that these values are for polymers with significantly lower surface areas and lower comonomer content than polymers reported previously in the literature.

Molecular Dynamics Simulations

Molecular dynamics simulations were performed to deduce the energetically most favorable structural conformations of

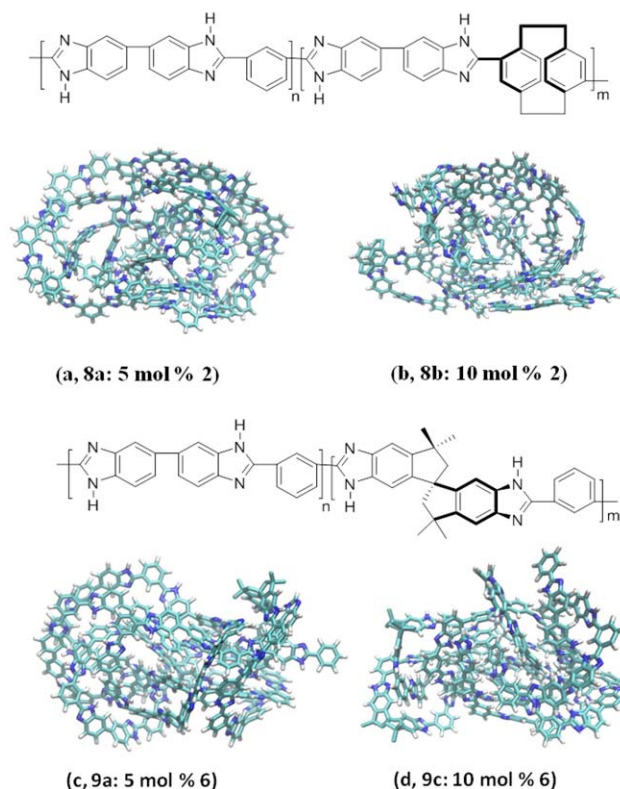


FIGURE 10 Molecular dynamics simulation of co-PBIs **8 a-b** and **9 a-c**. [Color figure can be viewed at wileyonlinelibrary.com]

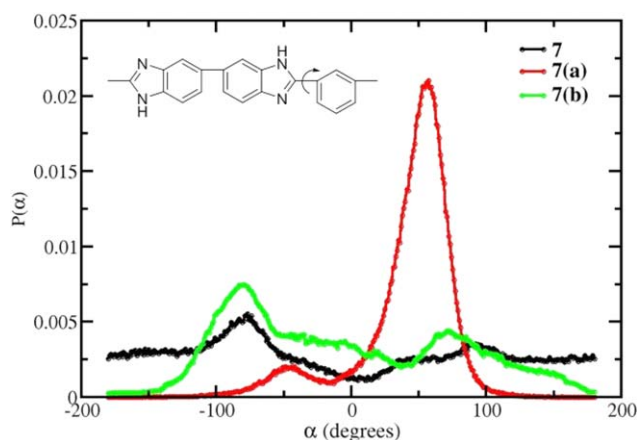


FIGURE 11 Distribution of dihedral angle of **7**, **7a**, and **7b** (structural representation is shown in inset). [Color figure can be viewed at wileyonlinelibrary.com]

PBIs. All-atomistic model of single chains with 24 repeat units were simulated at 800K. GROMACS package³⁸ and OPLS-AA³⁹ force field were used. The temperature chosen was ~ 50 – 60 K above the T_g ⁴⁰ of the polymers so as to ensure better sampling of polymer conformations. Energy minimized structures of a single chain of polymers along with the repeat units are shown in Figures 9 and 10 for compositions consisting of differing amounts of comonomers.

The energy minimized single chain of a homopolymer of PBI (**7**) shows a compact conformation [Fig. 9(a)]. In contrast, a PBI containing only comonomer **6** (**7a**) shows an open structure with large intra-molecular void space [Fig. 9(b)]. A similar result is also obtained with a PBI containing exclusively comonomer **2** (**7b**) [Fig. 9(c)]. The ability of the spiro monomer **6** and the cyclophane monomer **2** to pack poorly and create void space in the polymers can be seen clearly.

When the content of comonomer **6** is between 5 and 10 mol % in the copolymer, the distortion in polymer chain conformation is still very pronounced. A similar observation is also apparent when a cyclophane comonomer (**2**) is present in the copolymer [Fig. 10(a–d)].

To further characterize the conformation of the polymer chains, the radius of gyration (R_g) was calculated. The results are shown in Table 1. R_g values decrease in the order **9c** > **8b** > **9a** > **8a** > **7**, implying that the introduction of conformationally rigid comonomers with non-planar and contorted shapes in aromatic PBI backbone leads to expansion of the polymer chain. A probable reason for this may be the weakening of π – π interactions between aromatic groups of the PBI. This hypothesis further finds support from the fact that R_g of **8b** having benzene rings in the comonomer is lower than the R_g of **9c**, where the comonomer has only aliphatic linkages. R_g provides a qualitative measure of the rigidity of polymer chains.⁴¹ If a polymer is flexible, it will

possess larger degrees of conformational mobility resulting in the chain adopting a compact structure, whereas a polymer with a lower degree of conformational mobility will result in a more expanded chain. Thus, the observed order of conformational rigidity decreases in the order: **9c** > **8b** > **9a** > **8a** > **7**.

Another measure used to evaluate the rigidity of polymer chains in various simulation studies of organic molecules of intrinsic microporosity⁴² and PIMs^{43–45} is torsional angle distribution. Therefore, to further assess the conformational flexibility of PBIs (**7**, **7a**, and **7b**), torsional angle distribution of the dihedral angle connecting the monomer units in the chain were calculated (Fig. 11).

PBI **7a** shows a much narrower dihedral angle distribution compared with **7** and **7b** implying that polymer **7a** bearing a spirobisindane comonomer has a more rigid backbone with limited conformational mobility. More flexible polymers can span a wider conformational space leading to a broader distribution of dihedral angle values.⁴⁵ A correlation between rigidity and porosity is also indicated in previous experimental^{5,24,26} and simulation studies⁴⁶ on PIMs.

CONCLUSIONS

Co-PBIs were synthesized using a cyclophane monomer, 4,16-dicarboxyl[2.2]paracyclophane and a spirobisindane monomer, 5,5',6,6'-tetraamino-3,3,3',3'-tetramethyl-1,1'-spirobi[indane]. These monomers possess contorted and rigid structures and their incorporation in PBIs could lead to polymers with intrinsic porosities. The monomers and copolymers were synthesized and adequately characterized for their structure and composition. Copolymers with up to 10 mol % comonomers were soluble and could be processed into films. The copolymers were random in nature, amorphous, had high T_g , and high thermal stabilities. HR-TEM and nitrogen adsorption measurements provide evidence of mesoporous structures. The copolymers show enhanced carbon dioxide absorption and can be ascribed to its porous structure as well as the highly basic nature of the imidazole-nitrogen functionalized pore walls. Energetically most favorable structural conformation of the polymers was deduced from molecular dynamics simulations using an all-atomistic model and a chain length of 24 repeat units. The results show that the copolymer containing the cyclophane and the spirobisindane monomers has an open structure with large intramolecular void spaces. Thus, this work establishes the feasibility of synthesizing porous co-PBIs using a “bottoms-up” approach.

ACKNOWLEDGMENTS

This work was supported by CSIR under TAPSUN grant NWP0056-D; Bhatnagar Fellowship, CSIR, New Delhi (to S.S.); grant from Indian National Science Academy, New Delhi; research fellowship from UGC, India, (to V.K.); and post-doctoral research fellowship from CSIR, New Delhi (to S.C.).

REFERENCES AND NOTES

- 1 S. Qiu, T. Ben, *Porous Polymers: Design, Synthesis and Applications, Monographs in Supramolecular Chemistry No. 17*; The Royal Society of Chemistry: London, UK, **2016**.
- 2 D. Wu, F. Xu, B. Sun, R. Fu, H. He, K. Matyjaszewski, *Chem. Revs.* **2012**, *112*, 3959.
- 3 N. B. McKeown, P. M. Budd, *Chem. Soc. Rev.* **2006**, *35*, 675.
- 4 N. Chaoui, M. Trunk, R. Dawson, J. Schmidt, A. Thomas, *Chem. Soc. Rev.* **2017**, *46*, 3302.
- 5 N. B. McKeown, P. M. Budd, *Macromolecules* **2010**, *43*, 5163.
- 6 I. Rose, G. C. Bezzu, M. Carta, B. Comesaña-Gándara, E. Lasseuguette, M. C. Ferrari, P. Bernardo, G. Clarizia, A. Fuoco, J. C. Jansen, K. E. Hart, T. P. Liyana-Arachchi, C. M. Colina, N. B. McKeown, *Nat. Mater.* **2017**, *16*, 932.
- 7 T. Emmler, K. Heinrich, D. Fritsch, P. M. Budd, N. Chaukura, D. Ehlers, K. Rätzke, F. Faupel, *Macromolecules* **2010**, *43*, 6075.
- 8 Y. Iwakura, K. Uno, Y. Imai, *J. Polym. Sci. A.* **1964**, *2*, 2605.
- 9 E. W. Neuse, Aromatic Polybenzimidazoles. Synthesis, Properties, and Applications in Adv. Polym. Sci., In *Synthesis and Degradation Rheology and Extrusion*; H. J. Cantow, et al., Eds., Springer Berlin: Heidelberg, Germany, **1982**; Vol. 47, pp 1–42.
- 10 H. Vogel, C. S. Marvel, *J. Polym. Sci.* **1961**, *50*, 511.
- 11 S. Subianto, *Polym. Int.* **2014**, *63*, 1134.
- 12 J. S. Wainright, J. T. Wang, D. Weng, R. F. Savinell, M. J. Litt, *J. Electrochem. Soc.* **1995**, *142*, L121.
- 13 L. Xiao, H. Zhang, E. Scanlon, L. S. Ramanathan, E. W. Choe, D. Rogers, T. Apple, B. C. Benicewicz, *Chem. Mater.* **2005**, *17*, 5328.
- 14 J. S. Wainright, M. H. Litt and R. F. Savinell, *Handbook of Fuel Cells: Fundamentals, Technology and Applications*; W. Vielstich, A. Lamm, H. A. Gasteiger, Eds.; Wiley: Chichester, **2003**; Vol.3, p 436.
- 15 K. Y. Wang, T. S. Chung, J. J. Qin, *J. Membr. Sci.* **2007**, *300*, 6.
- 16 D. Mecerreyes, H. Grande, O. Miguel, E. Ochoteco, R. Marcilla, I. Cantero, *Chem. Mater.* **2004**, *16*, 604.
- 17 A. K. Sekizkardes, T. İslamoğlu, Z. Kahveci, H. M. El-Kaderi, *J. Mater. Chem. A.* **2014**, *2*, 12492.
- 18 D. Li, D. Shi, Y. Xia, L. Qiao, X. Li, H. Zhang, *ACS Appl. Mater. Interfaces* **2017**, *9*, 8742.
- 19 O. R. P. David, *Tetrahedron.* **2012**, *68*, 8977.
- 20 D. J. Cram, J. M. Cram, *Acc. Chem. Res.* **1971**, *4*, 204.
- 21 R. H. Gleiter, H. Hopf, Eds., *Modern Cyclophane Chemistry*, Wiley-VCH Publishers: Weinheim, Germany, **2004**.
- 22 R. A. Meyers, J. W. Hamersma, H. E. Green, *J. Polym. Sci. Lett.* **1972**, *10*, 685.
- 23 P. M. Budd, E. S. Elabas, B. S. Ghanem, S. Makhseed, N. B. McKeown, K. J. Msayib, C. E. Tattershall, D. Wang, *Adv. Mater.* **2004**, *16*, 456.
- 24 P. M. Budd, B. S. Ghanem, S. Makhseed, N. B. McKeown, K. J. Msayib, C. E. Tattershall, *Chem. Commun.* **2004**, 230.
- 25 X. Ma, R. Swaidan, Y. Belmabkhout, Y. Zhu, E. Litwiller, M. Jouiad, I. Pinnau, Y. Han, *Macromolecules* **2012**, *45*, 3841.
- 26 M. Carta, R. Malpass-Evans, M. Croad, Y. Rogan, J. C. Jansen, P. Bernardo, F. Bazzarelli, N. B. McKeown, *Science* **2013**, *339*, 303.
- 27 K. C. Stueben, *J. Polym. Sci. A.* **1965**, *3*, 3209.
- 28 V. Molteni, D. Rhodes, K. Rubins, M. Hansen, F. D. Bushman, J. S. Siegel, *J. Med.Chem.* **2000**, *43*, 2031.
- 29 M. Mizuno, M. Yamano, *Org. Lett.* **2005**, *7*, 3629.
- 30 S. Maity, T. Jana, *Polym. Int.* **2015**, *64*, 530.
- 31 A. Sannigrahi, S. Gosh, J. Lalnunluanga, T. Jana, *J. Appl. Polym. Sci.* **2009**, *111*, 2194.
- 32 K. S. W. Sing, D. H. Evertt, R. A. W. Haul, L. Moscou, R. A. Pierotti, J. Rouquerol, T. Siemieniowska, *Pure & Appl. Chem.* **1985**, *4*, 603.
- 33 H. Yu, M. Tian, C. Shen, Z. Wang, *Polym. Chem.* **2013**, *4*, 961.
- 34 Y. C. Zhao, T. Wang, L. Zhang, Y. Cuia, B. Han, *Polym. Chem.* **2015**, *6*, 748.
- 35 M. G. Rabbani, H. M. El-Kaderi, *Chem. Mater.* **2012**, *24*, 1511.
- 36 G. Li, B. Zhang, J. Yan, Z. Wang, *J. Mater. Chem. A.* **2016**, *4*, 11453.
- 37 R. Ullah, M. Atilhan, A. Diab, E. Deniz, S. Aparicio, C. Yavuz, *T. Adsorption.* **2016**, *22*, 247.
- 38 B. Hess, C. Kutzner, D. van der Spoel, E. Lindahl, *J. Chem. Theory Comput.* **2008**, *4*, 435.
- 39 W. L. Jorgensen, D. S. Maxwell, J. Tirado-Rives, *J. Am. Chem. Soc.* **1996**, *118*, 11225.
- 40 H. A. Schneider, E. A. Di Marzio, *Polymer* **1992**, *33*, 3453.
- 41 M. Rubinstein, R. H. Colby, *Polymer Physics*. Oxford University Press: London, UK, **2003**.
- 42 L. J. Abbott, N. B. McKeown, C. M. Colina, *J. Mater. Chem. A.* **2013**, *1*, 11950.
- 43 E. Tocci, L. De Lorenzo, P. Bernardo, G. Clarizia, F. Bazzarelli, N. B. McKeown, M. Carta, R. Malpass-Evans, K. Friess, K. Pilnáček, M. Lanč, Y. P. Yampolskii, L. Strarannikova, V. Shantarovich, M. Mauri, J. C. Jansen, *Macromolecules* **2014**, *47*, 7900.
- 44 Y. Chen, L. Chen, K. Chang, T. Chen, Y. Lin, K. Tung, *J. Membr. Sci.* **2016**, *514*, 114.
- 45 T. M. Madkour, *J. Phys.: Conf. Ser.* **2013**, *454*, 012037.
- 46 K. E. Hart, L. J. Abbott, N. B. McKeown, C. M. Colina, *Macromolecules* **2013**, *46*, 5371.